TEXAS
The University of Texas at Austin

Staged Strategy to Avoid Hospital Surge and Preventable Mortality, while Reducing the Economic Burden of Social Distancing

Daniel Duque, Mauricio Tec, David P. Morton, James Scott, Haoxiang Yang, Remy Pasco, Kelly Pierce, Spencer J. Fox, Michael Pignone, Parker Hudson, Lauren Ancel Meyers

The University of Texas at Austin
COVID-19 Modeling Consortium

utpandemics@austin.utexas.edu

Staged Strategy to Avoid Hospital Surge and Preventable Mortality, while Reducing the Economic Burden of Social Distancing Measures

Presented to the city of Austin and Travis County on May 18, 2020

The University of Texas COVID-19 Modeling Consortium

Contributors: Daniel Duque, Mauricio Tec, David P. Morton, James Scott, Haoxiang Yang, Remy Pasco, Kelly Pierce, Spencer J. Fox, Michael Pignone, Parker Hudson, Lauren Ancel Meyers

Contact: utpandemics@austin.utexas.edu

Background

In order to balance the goals of preventing death from COVID-19 while also minimizing other negative (societal and economic) impacts, it is important to have a clear monitoring strategy that can guide public policy. Such a strategy can be used to help guide the application of the range of non-pharmacological interventions that have been shown to reduce disease transmission and death. Here, we propose a coherent data-driven strategy for triggering both the tightening and relaxation of policies to ensure COVID-19 hospitalizations do not exceed healthcare capacity in cities while minimizing the duration of restrictions on commerce, healthcare, recreation, and schooling.

As US states reopen during the COVID-19 pandemic, it is expected that cases will increase. The goal of this strategy is to reduce economic hardship while maintaining access to hospital care for both COVID-19 patients and all other patients and to avoid excess serious complications or death for those with COVID-19 or for those with other medical conditions like cancer or cardiovascular disease, who may not receive timely or safe care if health system overwhelmed by COVID-19. In addition, an overwhelmed health system creates a more dangerous environment for our health care providers who will be more likely to be infected and hence exacerbate health care shortages. It could also seriously compromise the public confidence in their health and safety.

Thresholds

Policy makers have proposed to track several data streams throughout the COVID-19 pandemic and initiate reopening policies when specific epidemiological thresholds are achieved, including: flu-like illness syndromic surveillance, case counts, deaths, test and trace metrics, and hospital capacity (Table A). The reliability and timeliness of each of these sources has been variable across time and jurisdiction. Until COVID-19 testing capacity and priorities stabilize, COVID-19 hospital admissions will likely provide the best balance of accuracy and timeliness for determining when to pause, brake, or accelerate reopening policies.

Proposed Strategy

Given the goal of preventing a hospital surge that overwhelms the health system leading to excess death, the daily new COVID-19 hospital admissions (7-day rolling average) is a reliable indicator of impending hospital surge and can be used to trigger the tightening and relaxation of reopening policies. Most importantly, the strategy we propose could be flexibly tailored to individual metropolitan areas–based on local demographic characteristics, COVID-19 threat level, and healthcare capacity–so that US states can develop data-driven and regionalized plans.

COVID-19 hospital admissions can be used to rapidly gauge the speed of COVID-19 transmission and project the future trajectory of pandemic waves in a community. Through modeling, we can determine for each region a “trigger” for when a surge is coming, which would indicate the need for a “hard brake” - a strict shelter-in-place order may be required. We can also adjust staged reopening plans based on clear thresholds in daily hospital admissions to avoid reaching a point where a full-blown stay-home measure is “triggered”. This strategy is complementary to our efforts to guide social distancing, wearing of face masks, and increase testing and tracing, as these are essential to driving down the effective reproduction number of the virus (R_e).

To implement this strategy, we need two critical pieces of data:

1. Safe hospital capacity in each region or metropolitan area

2. New, daily, confirmed, hospital admissions for individuals requiring care for COVID-19

Austin Area Case Study

Tracking Daily COVID-19 Hospital Admissions to Estimate Transmission

Daily admissions data currently provides the most reliable, though slightly delayed, indicator of the changing rate of spread. We calculate that Austin's shelter-in-place order reduced COVID-19 transmission by at least 75%, bringing the reproduction number R_e well below one. Since May 1, we estimate that the reproduction number has been steadily rising towards one (Figure 1).

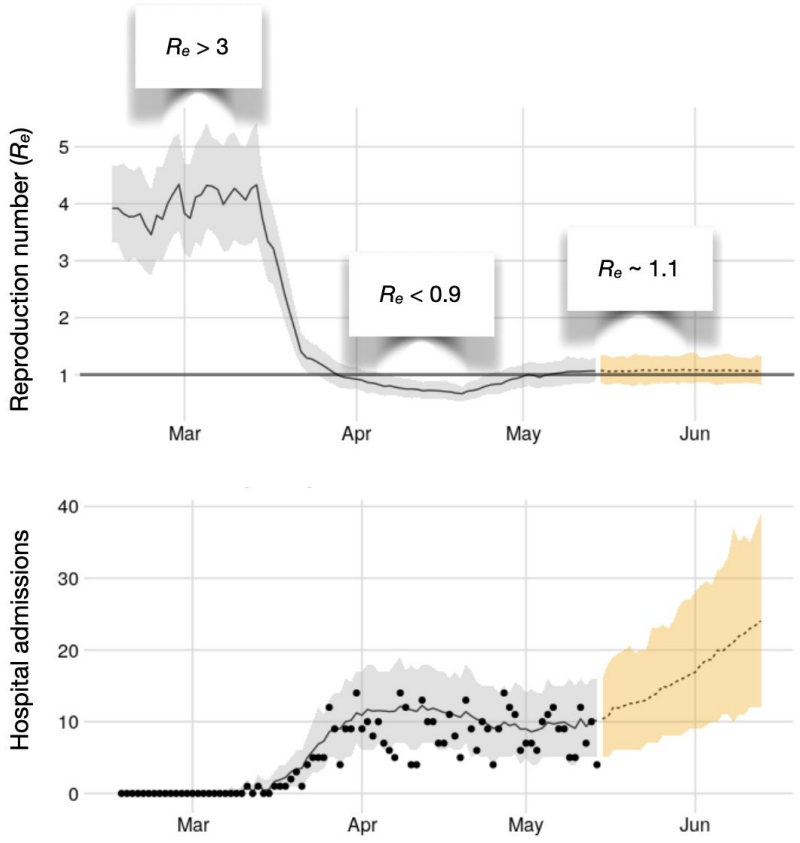

Figure 1. Tracking COVID-19 transmission by monitoring daily, new COVID-19 hospital admissions (Austin example)

Scenario 1 – Maintain 50% Reopening

Based on our most recent projections for COVID-19 transmission in Austin, we project that Austin will experience a hospital surge starting in June that will exceed hospital capacity this summer, unless stricter measures are enacted (Figure 2). Note that this scenario assumes that **strict** measures are taken to reduce the risk of COVID-19 transmission in high risk populations.

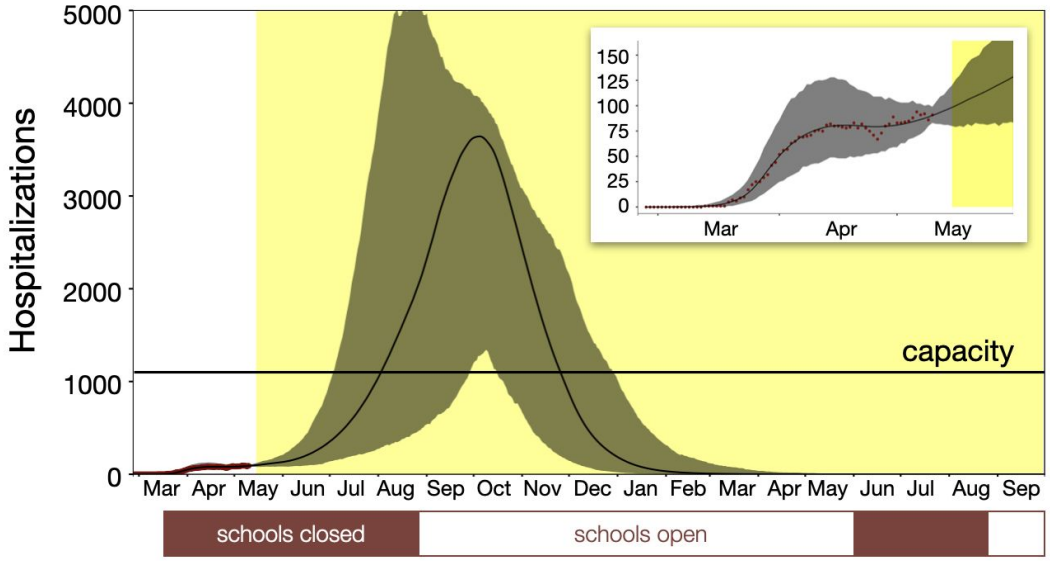

Figure 2. Projected COVID-19 hospital surge in Austin assuming that transmission rebounds by 50% following the May 1, 2020 reopening and high risk populations remain 'strictly cocooned'. This assumes that intervention policies continue to reduce transmission by over 60% relative to the baseline reproduction number observed in early March before stay-home orders began.

Scenario 2 – Reopen until surge trigger

The strategy that would avoid a hospital surge AND minimize the total number of days of “lockdown” (March shelter-in-place level of restrictions) would re-enter lockdown if the “trigger” of 45 new daily COVID-19 patients was reached in the Austin MSA (Figure 3). Of note, this strategy would be expected to require four lockdown periods, each lasting three to six weeks, between now and spring of 2021. This strategy would allow us to cautiously reopen commerce and schools in the intervening periods, with “herd immunity” eventually achieved in late 2021, in the absence of an effective vaccine.

Although there may be a high level of societal resistance to these additional shelter-in-place periods, it is important to emphasize that there is a “point of no return” that if we cross, we must put hard brakes on reopening to avert overwhelming hospital surges. This trigger should be communicated clearly.

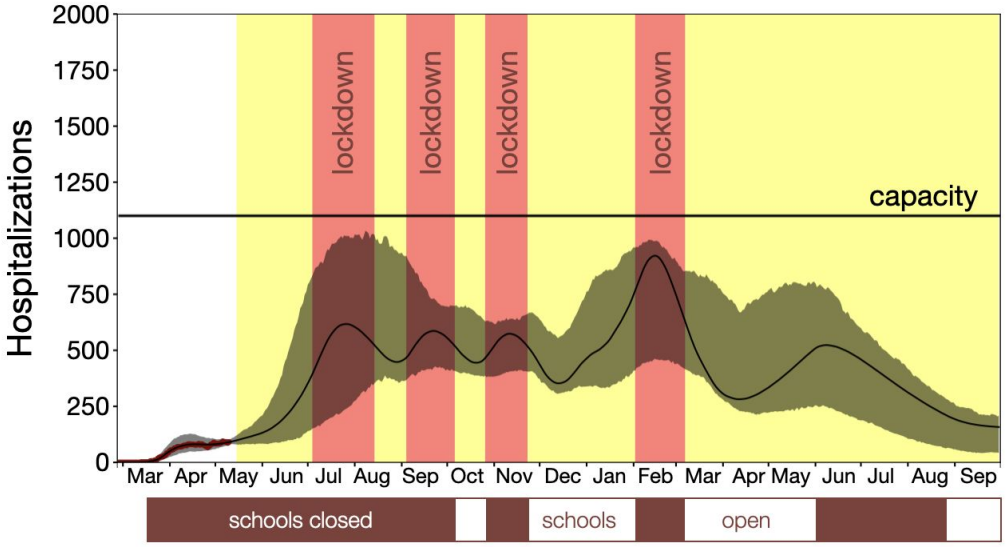

Figure 3. Projected COVID-19 hospitalization in Austin under a single trigger policy that enacts strict stay-home measures to prevent catastrophic hospital surges. Measures are enacted and relaxed when the 7-day rolling average of daily COVID-19 hospital admissions exceed or drop below a unique threshold determined for each metropolitan area. For Austin, this threshold is 45 new patients.

Scenario 3 – Flexible Reopening

The flexible strategy would allow multiple stages of reopening. Moving between stages (braking or accelerating) would be guided by the number of daily hospital COVID-19 admissions in a region to prevent both a “surge” with excess mortality and reduce the need for a full “stay at home” order.

In the example of Austin, these intermediate triggers allow the city to remain in stages 2, 3 and 4 of opening and considerably reduce the need for shelter-in-place orders (Figure 4). We would expect to get to the “point of no return” once in the fall of 2020, requiring approximately one month of sheltering-in-place.

Importantly this approach would be specific to each metropolitan area, so other cities could accelerate or brake independent of Austin, once the triggering models have been created for other metropolitan areas. Communicating this strategy to the public could help create support to follow our social distancing and reopening guidelines and allow businesses to anticipate changes in both opening and braking specific to their local community. If communities follow such social distancing guidance while increasing testing, tracing and isolation efforts to reduce transmission, we may never reach thresholds for full-fledged “lockdowns”.

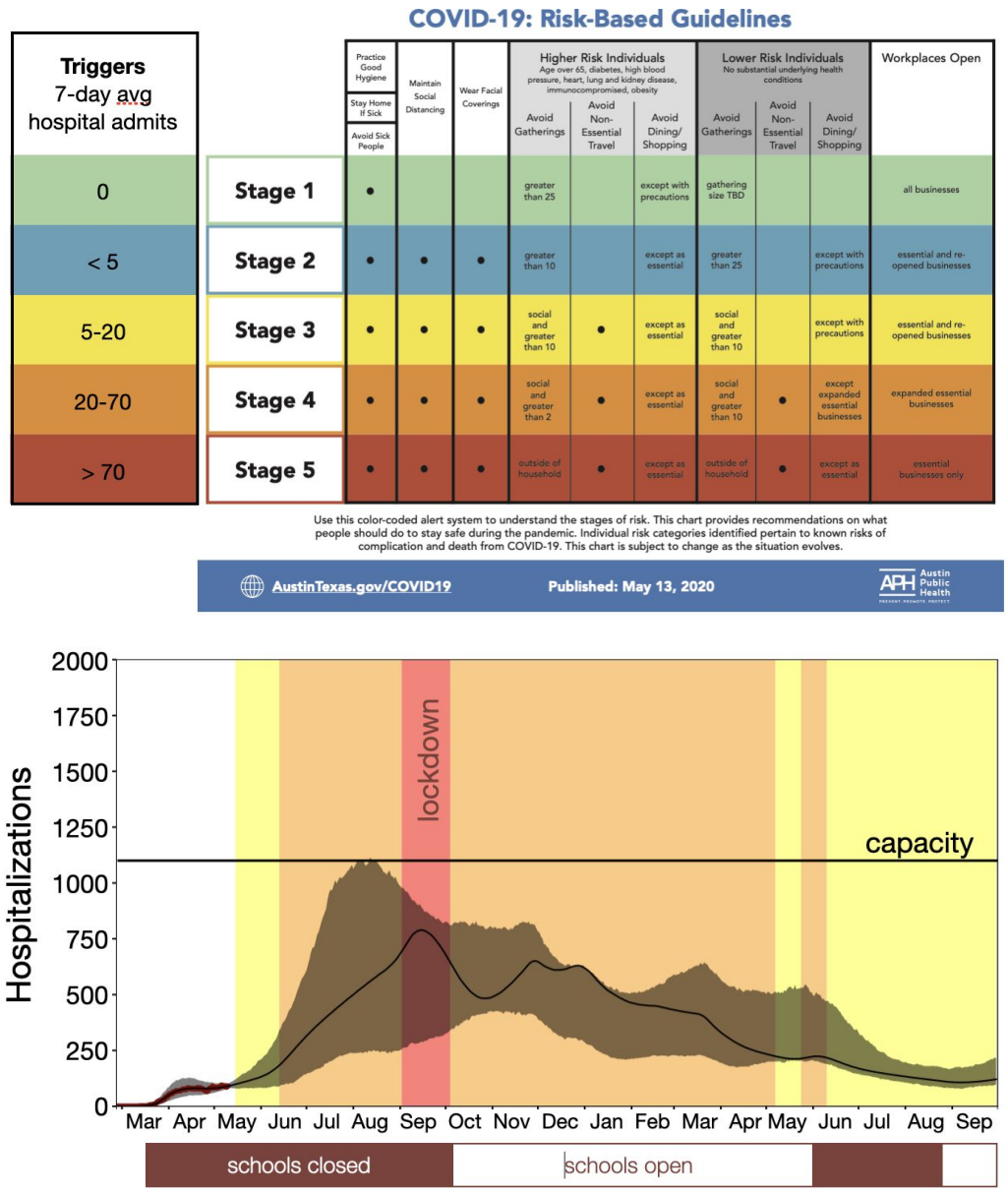

Figure 4. A multi-stage policy in which the city of Austin toggles the alert level when the 7-day rolling average of new COVID-19 hospital admissions crosses specific thresholds. The table above gives the triggers for Austin's recently-posted risk levels [1]. The projected COVID-19 hospitalization in Austin under this multi-trigger policy toggles between intermediate levels of re-opening to prevent lengthy shelter-in-place orders.

Summary

New, daily, confirmed COVID-19 hospital admissions is an important measure to follow during reopening to prevent a hospital surge and excess deaths. It allows calculation of the community effective reproduction number (R_e) and the determination of trigger/thresholds to allow a flexible, regional, data-driven reopening plan. The next steps needed for other areas to use this approach are to share new, daily, confirmed COVID-19 admissions and report their safe-level, regional hospital capacity.

Appendix

Table A. Proposed measures for relaxing shelter-in-place policies

Potential Measure	Potential thresholds	Advantages	Disadvantages	Notes
Influenza-like Illness (ILI) Syndromic Surveillance	Stable or Decreasing ILI for 2 weeks	May be earliest measure of increase cases	Many causes of ILI especially in fall/winter	Publicly reported data or use of COVID-19 symptom checker data
Case Count	Stable or Decreasing case counts for 2 weeks	Most closely reflects changes in infections; shortest lag between infection and reporting	Subject to bias based on changes in testing: capacity, priority populations, locations, reporting. Lags infections by at least 6+ days if primarily testing symptomatic cases.	Cases vary in risk of bad outcomes and transmission
Test Capacity	Daily per capita testing >0.1% population	Correlates with testing coverage that has achieved control in other countries	Higher prevalence will require more testing likely >0.15% population per day	
Test positivity rate	<5-10%	Allows for partial correction of changes in testing volume	Can be biased if testing is directed based on risk	Increase preoperative testing in very low risk group
Contact Tracing	>90% cases investigated >80% contacts traced	Finds new cases early and prevents spread	Lapses in quarantine or isolation threaten validity	Time dependent, ideally <48 hours
Hospital capacity	>20% Hospital & ICU beds	Closely tracks with risk of adverse outcomes	Difficult to define safe levels	Capacity can change quickly based

	available for surge			on surgical volumes
COVID Deaths	Stable or decreasing deaths for 2 weeks	Easier to count	Attribution can be challenging; Lags other measures	
Total (excess) deaths	Return to baseline from historical controls	Easiest to count	Lags other measures; Hard to determine excess over expected	Assumes all excess due to COVID-19
New COVID-19 Admissions*	Trigger based on regional hospital capacity	Less subject to bias than case-based measures and total hospitalizations; Identifies important spectrum of disease	Lags infections by 10+ days; Harder to manage data	See Strategy Above

COVID-19 Epidemic Model Structure and Parameters

The model structure is diagrammed in Figure A1 and described in the equations below.
For each age and risk group, we build a separate set of compartments to model the transitions between the states: susceptible (S), exposed (E), pre-symptomatic infectious (P^Y), pre-asymptomatic infectious (P^A), symptomatic infectious (I^Y), asymptomatic infectious (I^A), symptomatic infectious that are hospitalized (I^H), recovered (R), and deceased (D). The symbols S, E, P^Y, P^A ,I^Y, I^A, I^H, R, and D denote the number of people in that state in the given age/risk group and the total size of the age/risk group is

$$N = S + E + P^Y + P^A + I^Y + I^A + I^H + R + D.$$

The model for individuals in age group a and risk group r is given by:

$$\frac{dS_{a,r}}{dt} = -S_{a,r} \cdot \sum_{i \in A} \sum_{j \in K} (I^Y_{i,j}\omega^Y + I^A_{i,j}\omega^A + P^Y_{i,j}\omega^{PY} + P^A_{i,j}\omega^{PA})\beta\phi_{a,i}/N_i$$

$$\frac{dE_{a,r}}{dt} = S_{a,r} \cdot \sum_{i \in A} \sum_{j \in K} (I^Y_{i,j}\omega^Y + I^A_{i,j}\omega^A + P^Y_{i,j}\omega^{PY} + P^A_{i,j}\omega^{PA})\beta\phi_{a,i}/N_i - \sigma E_{a,r}$$

$$\frac{dP^A_{a,r}}{dt} = (1-\tau)\sigma E_{a,r} - \rho^A P^A_{a,r}$$

$$\frac{dP^Y_{a,r}}{dt} = \tau\sigma E_{a,r} - \rho^Y P^Y_{a,r}$$
$$\frac{dI^A_{a,r}}{dt} = \rho^A P^A_{a,r} - \gamma^A I^A_{a,r}$$
$$\frac{dI^Y_{a,r}}{dt} = \rho^Y P^Y_{a,r} - (1-\pi)\gamma^Y I^Y_{a,r} - \pi\eta I^Y_{a,r}$$
$$\frac{dI^H_{a,r}}{dt} = \pi\eta I^Y_{a,r} - (1-\nu)\gamma^H I^H_{a,r} - \nu\mu I^H_{a,r}$$
$$\frac{dR_{a,r}}{dt} = \gamma^A I^A_{a,r} + (1-\pi)\gamma^Y I^Y_{a,r} + (1-\nu)\gamma^H I^H_{a,r}$$
$$\frac{dD_{a,r}}{dt} = \nu\mu I^H_{a,r}$$

where A and K are all possible age and risk groups, ^{A}, ^{Y}, ^{PA}, ω^{PY} are the relative infectiousness of the I^A, I^Y, I^{PA}, I^{PY} compartments, respectively, β is transmission rate, $_{a,i}$ is the mixing rate between age group a, $i \in A$, ^{A}, ^{Y}, ^{H} are the recovery rates for the I^A, I^Y, I^H compartments, respectively, σ is the exposed rate, ρ^A, ρ^Y are the pre-(a)symptomatic rates, τ is the symptomatic ratio, π is the proportion of symptomatic individuals requiring hospitalization, η is rate at which hospitalized cases enter the hospital following symptom onset, ν is mortality rate for hospitalized cases, and μ is rate at which terminal patients die.

We model stochastic transitions between compartments using the τ-leap method [2,3] with key parameters given in Tables A1-3. Assuming that the events at each time-step are independent and do not impact the underlying transition rates, the numbers of each type of event should follow Poisson distributions with means equal to the rate parameters. We thus simulate the model according to the following equations:

$$S_{a,r}(t+1) - S_{a,r}(t) = -P_1$$
$$E_{a,r}(t+1) - E_{a,r}(t) = P_1 - P_2$$
$$P^A_{a,r}(t+1) - P^A_{a,r}(t) = (1-\tau)P_2 - P_3$$
$$P^Y_{a,r}(t+1) - P^Y_{a,r}(t) = \tau P_2 - P_4$$
$$I^A_{a,r}(t+1) - I^A_{a,r}(t) = P_3 - P_5$$
$$I^Y_{a,r}(t+1) - I^Y_{a,r}(t) = P_4 - P_6 - P_7$$
$$I^H_{a,r}(t+1) - I^H_{a,r}(t) = P_7 - P_8 - P_9$$
$$R_{a,r}(t+1) - R_{a,r}(t) = P_5 + P_6 + P_8$$

with

$$P_1 \sim \text{Pois}(S_{a,r}(t)F_{a,r}(t))$$
$$P_2 \sim \text{Pois}(\sigma E_{a,r}(t))$$

$$P_3 \sim \text{Pois}(\rho^A P^A_{a,r}(t))$$
$$P_4 \sim \text{Pois}(\rho^Y P^Y_{a,r}(t))$$
$$P_5 \sim \text{Pois}(\gamma^A I^A_{a,r}(t))$$
$$P_6 \sim \text{Pois}((1-\pi)\gamma^Y I^Y_{a,r}(t))$$
$$P_7 \sim \text{Pois}(\pi\eta I^Y_{a,r}(t))$$
$$P_8 \sim \text{Pois}((1-\nu)\gamma^H I^H_a)$$
$$P_9 \sim \text{Pois}(\nu\mu I^H_{a,r}(t))$$

and where $F_{a,r}$ denotes the force of infection for individuals in age group a and risk group r and is given by:

$$F_{a,r}(t) = \sum_{i\in A}\sum_{j\in K}(I^Y_{i,r}(t)\omega^Y + I^A_{i,r}(t)\omega^A + P^Y_{i,j}(t)\omega^{PY} + P^A_{i,j}(t)\omega^{PA})\beta_{a,i}\phi_{a,i}/N_i$$

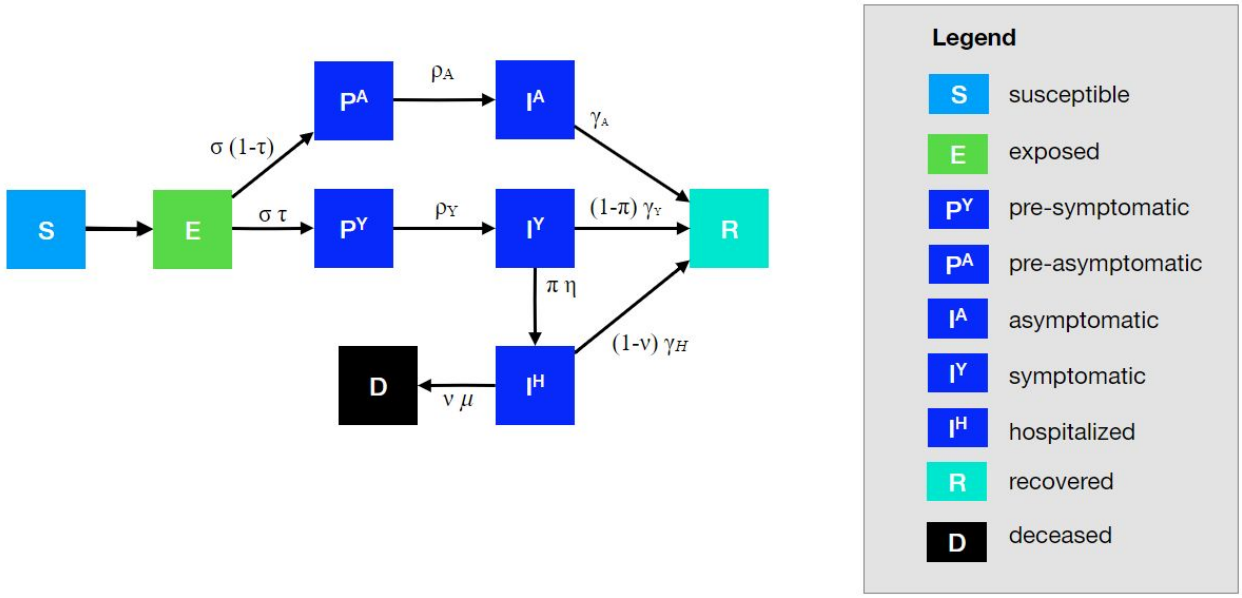

Figure A1. Compartmental model of COVID-19 transmission in a US city. Each subgroup (defined by age and risk) is modeled with a separate set of compartments. Upon infection, susceptible individuals (*S*) progress to exposed (*E*) and then to either pre-symptomatic infectious (P^Y) or pre-asymptomatic infectious (P^A) from which they move to symptomatic infectious (I^Y) and asymptomatic infectious (I^A) respectively. All asymptomatic cases eventually progress to a recovered class where they remain protected from future infection (*R*); symptomatic cases are either hospitalized (I^H) or recover. Mortality (*D*) varies by age group and risk group and is assumed to be preceded by hospitalization.

Real-time estimation of R_e

We estimate the daily effective reproduction number (R_e) through statistical fitting of our stochastic model to hospital admit, discharge, and mortality data. To fit our model to these data from the Austin MSA we adapted the model described above in three important ways: (1) we allow the transmission rate to be informed by local social mobility data, (2) we allow the hospital discharge rate to change through time according to an AR(1) process, and (3) we use a single, average daily contact matrix that is the weighted mean between the weekend and weekday contact matrices used in the model above. In this way we allow our model to be driven primarily through mobility patterns from the data, rather than assumptions regarding expected contacts in different locations.

Model fitting was conducted through iterated filtering using the pomp package in R to obtain maximum likelihood estimates for all fitted parameters [4,5]. We carried out particle filtering using the fitted parameters to obtain smoothed daily posterior distribution estimates for all state variables including $\beta(t)$, which we then can use to calculate R_e using the next-generation estimation method with our fitted parameters.

Trigger Threshold Selection Methods

We optimize the timing of when to initiate different stages of reopening, guided by triggers that monitor both daily new-hospital admissions and total hospitalizations. Triggering to a stage corresponding to a tighter lockdown occurs when a seven-day moving average of daily hospital admissions grows to exceed an optimized threshold. Moving to a more relaxed stage occurs when: (a) the same moving average drops below the level threshold and (b) total hospitalizations are under a safety threshold. Each stage corresponds to a percentage of reduction in transmission, school closure, and a cocooning level for the high-risk population.

In addition to epidemiological constraints governing the transmission and severity of the virus, our optimization model selects triggers that ensure the aggregate daily arrival rate of new patients to hospitals is such that, with high probability, the demand for hospital beds does not exceed supply. We use the square-root staffing rule of [6] for an M/M/s queue. The parameter of this queue is set up to ensure a probability of over 0.99997 for a single arriving patient to have a bed when admitted. We assume that imposing stage k is associated with a daily socio-economic cost, c^k, and we propose an optimization model that seeks trigger thresholds to minimize the total cost to the model's horizon.

The optimization framework we use follows that in [7], with distinctions in the following three details:

1. *Higher fidelity simulation model:* In particular, we use the updated simulation model as shown in Figure A1, which adds pre-symptomatic and pre-asymptomatic compartments. Parameters are updated as well according to Table A1-A4. These equations correspond

to the dynamical equations labeled Constraints (1) in Duque et al. [7], and here we name them “simulation model constraints.”

2. *Multiple stages versus single stage*: In [7], we can toggle between two states using a threshold, , which can adapt over time, as well as the hospitalization safety threshold, . In the current multi-stage model, we fix r to be 60% of the hospital capacity.

   Furthermore, we search for a set of stage thresholds, l^k , where $k \in K$ indexes the stages for increasingly strident levels of risk reduction. Stage k is executed when either of the following criteria are met. (These are similar to Constraints (2) in reference [7], and we name them “stage determination criteria.”): (1) Increase (tighten) the stage: The 7-day moving average of hospitalization admissions exceeds stage k’s threshold, and the current stage $k-1$ has been executed for longer than the minimum length (i.e., 14 days in our implementation); (2) Decrease (relax) the stage: The 7-day moving average of hospitalization admissions is smaller than the current stage $k+1$’s threshold, the current hospitalization number is below safety threshold, r, and the current stage $k+1$ has been executed for longer than the minimum length (14 days). We can define the indicator variables X_t^k as:

$$X_t^k = \begin{cases} 1 & if\ stage\ k\ is\ executed\ at\ time\ t \\ 0 & otherwise \end{cases},$$

   and the optimization model can be written as:

$$\begin{aligned} \min_{l^k} \quad & E_\omega \sum_{t\in\mathcal{T}} \sum_{k\in K} c^k X_t^k \\ s.t. \quad & \{l^k\}_{k\in K} \in \mathcal{F} \\ & Simulation\ model\ constraints \\ & Stage\ determination\ criteria \end{aligned}$$

   The collection of feasible sets of thresholds, , is defined as follows:

   . $l^{|K|+1} = +\infty$

   . $0 \le l^k \le l^{k+1} \quad \forall k \in K$

   · With the sample path corresponding to a point forecast (i.e., model (3) in [7], the daily hospitalizations obtained must satisfy the square-root staffing rule.

3. *Chance constraint and optimality criterion*: In reference [7], we consider the candidate set of thresholds feasible as long as a chance constraint is met, i.e., the probability that the number of “heads in beds” exceeds hospital capacity is below a specified level. Here, we revise our selection rules for an optimal set of thresholds as follows:
   a. First, among thresholds satisfying the chance constraint defined as inequality (4e) in reference [7], we select the one with the lowest expected cost;
   b. Second, if the chance constraint is infeasible we select thresholds with the smallest violation of the chance constraint. If there is a tie in the violation, we select a solution with the lowest expected cost.

Estimating the effect of the Stay Home-Work Safe order

We estimated the transmission rate of COVID-19 in the Austin-Round Rock MSA before and after the March 24th *Stay Home-Work Safe* order using least-squares fitting, which compares the predicted and observed numbers of daily hospitalizations (i.e., heads in beds) for the Austin-Round Rock MSA. We assume that: (i) the epidemic starts with a single case on February 15, 2020 with an initial transmission rate of β, (ii) the transmission rate decreases when school closures are enacted on March 19, 2020 (by an amount determined by our pre-set contact matrices), (iii) the transmission rate decreases further by an amount d_1 on March 25th following the *Stay Home-Work Safe* order.

We estimate d_1 using a nonlinear least squares fitting procedure in the SciPy/Python package across a range of possible start dates [8]. For a given start date, we run a deterministic simulation of our model assuming a central value for d_1. Using a trust region method, the algorithm finds value of d_1 that minimize the sum of squared daily differences between the simulated ($\hat{H}_t$) and actual (H_t) daily hospitalizations from March 13 through April 19 2020: for the assumed start date as $S(d) = \sum_t (H_t - \hat{H}_t)^2$. We then select the simulation start date that produces the lowest normalized mean square deviation and fix that start date for subsequent simulations. For the Austin-Round Rock MSA, the best-fit simulation start date is February 27, 2020. Mobility data indicate that the Austin-Round Rock MSA experiences an increase in social interaction on approximately April 20, 2020 (Safegraph data, not shown). We use least squares fitting to estimate a second transmission reduction value, d_2, *after fixing our estimates for* β, d_1, and the best simulation start date.

Table A1. Initial conditions, school closures and social distancing policies

Variable	**Settings**
Initial day of simulation	2/27/2020
Initial infection number in locations	1 pre-symptomatic case in 18-49y age group
School closure	3/15/2020 - 8/17/2020. After 8/17/2020: scenario-specific or policy-specific
Age-specific and day-specific contact rates	Home, work, other and school matrices provided in Tables S4.1-S4.4, and are modified to reflect school closures and other changes in contact patterns and transmission rates during simulations

Table A2. Model parameters[a]

Parameters	Best guess values	Source
β: baseline transmission rate	0.0615	Fitted to daily COVID-19 hospitalizations in Austin-Round Rock MSA
κ: reduction in transmission	From 2020-02-27 to 2020-03-24: 0 From 2020-03-25 to 2020-04-19: 0.78 From 2020-04-20 to 2020-05-10: 0.72 After 2020-05-11: Depends on the policy	From 2020-03-25 to 2020-05-10: fitted to daily COVID-19 hospitalizations in Austin-Round Rock MSA
γ^A: recovery rate on asymptomatic compartment	Equal to γ^Y	
γ^Y: recovery rate on symptomatic non-treated compartment	$\frac{1}{\gamma^Y} \sim \ Triangular\,(3.0, 4.0, 5.0)$	He et al. [9]
τ: symptomatic proportion (%)	57	Gudbjartsson et al. [10]
σ: exposed rate	$\frac{1}{\sigma} \sim \ Triangular\,(1.9, 2.9, 3.9)$	Based on incubation [11] and pre-symptomatic periods
ρ^A: pre-asymptomatic rate	Equal to ρ^Y	
ρ^Y: pre-symptomatic rate	$\frac{1}{\rho^Y} = 2.3$	He et al. [9]
P: proportion of pre-symptomatic transmission (%)	44	He et al. [9]
ω^Y: relative infectiousness of symptomatic individuals	1.0	By construction
ω^P: relative infectiousness of pre-symptomatic individuals	$\omega^P = \frac{P}{1-P}\frac{\tau\omega^Y\left[YHR/\eta + (1-YHR)/\gamma^Y\right] + (1-\tau)\omega^A/\gamma^A}{\tau\omega^Y/\rho^Y + (1-\tau)\omega^A/\rho^A}$ $\omega^{PY} = \omega^P\omega^Y, \omega^{PA} = \omega^P\omega^A$	
ω^A: relative infectiousness of infectious individuals in compartment I^A	$\omega_A \sim Triangular(0.29, 0.29, 1.4)$	$\frac{1}{\omega_A}$:1.5 (95% CI: 0.7-3.4) from He et al. [12]
IFR: infected fatality ratio, age specific (%)	Low risk: [0.0009167, 0.002179, 0.03388, 0.2520, 0.6440] High risk:[0.009167, 0.02179, 0.3388, 2.520, 6.440]	Age adjusted from Verity et al. [13]

YFR: symptomatic fatality ratio, age specific (%)	Low risk: [0.001608, 0.003823, 0.05943, 0.4420, 1.130] High risk: [0.01608, 0.03823, 0.5943, 4.420, 11.30]	$YFR = \frac{IFR}{\tau}$
h: high-risk proportion, age specific (%)	[8.2825, 14.1121, 16.5298, 32.9912, 47.0568]	Estimated using 2015-2016 Behavioral Risk Factor Surveillance System (BRFSS) data with multilevel regression and poststratification using CDC's list of conditions that may increase the risk of serious complications from influenza[14–16]

[a]Values given as five-element vectors are age-stratified with values corresponding to 0-4, 5-17, 18-49, 50-64, 65+ year age groups, respectively.

Table A3 Hospitalization parameters

Parameters	Value	Source
γ^H: recovery rate in hospitalized compartment	$\frac{1}{\gamma^H} \sim Triangular(9.4, 10.7, 12.8)$	Fit to Austin admissions and discharge data (Avg=10.96. 95% CI = 9.37 to 12.76)
YHR: symptomatic case hospitalization rate (%)	Low risk: [0.04021, 0.03091, 1.903, 4.114, 4.879] High risk: [0.4021, 0.3091, 19.03, 41.14, 48.79]	Age adjusted from Verity et al. [13]
π: rate of symptomatic individuals go to hospital, age-specific	$\pi = \frac{\gamma^Y * YHR}{\eta + (\gamma^Y - \eta)YHR}$	
η: rate from symptom onset to hospitalized	0.1695	5.9 day average from symptom onset to hospital admission Tindale et al.[17]
μ: rate from hospitalized to death	$\frac{1}{\mu} \sim Triangular(5.2, 8.1, 10.1)$	Fit to Austin admissions and discharge data (Avg=7.8, 95% CI = 5.21 to 10.09)
HFR: hospitalized fatality ratio, age specific (%)	[4, 12.365, 3.122, 10.745, 23.158]	$HFR = \frac{YFR}{YHR}$
ν: death rate on hospitalized individuals, age specific	$\nu = \frac{\gamma^H HFR}{\mu + (\gamma^H - \mu)HFR}$	
Healthcare capacity	Hospital beds: 1,100 (for COVID-19 patients only)	Estimates provided by each of the region's hospital systems and aggregated by regional public health leaders

Table A4.1 Home contact matrix. Daily number contacts by age group at home.

	0-4y	5-17y	18-49y	50-64y	65y+
0-4y	0.5	0.9	2.0	0.1	0.0
5-17y	0.2	1.7	1.9	0.2	0.0
18-49y	0.2	0.9	1.7	0.2	0.0
50-64y	0.2	0.7	1.2	1.0	0.1
65y+	0.1	0.7	1.0	0.3	0.6

Table A4.2 School contact matrix. Daily number contacts by age group at school.

	0-4y	5-17y	18-49y	50-64y	65y+
0-4y	1.0	0.5	0.4	0.1	0.0
5-17y	0.2	3.7	0.9	0.1	0.0
18-49y	0.0	0.7	0.8	0.0	0.0
50-64y	0.1	0.8	0.5	0.1	0.0
65y+	0.0	0.0	0.1	0.0	0.0

Table A4.3 Work contact matrix. Daily number contacts by age group at work.

	0-4y	5-17y	18-49y	50-64y	65y+
0-4y	0.0	0.0	0.0	0.0	0.0
5-17y	0.0	0.1	0.4	0.0	0.0
18-49y	0.0	0.2	4.5	0.8	0.0
50-64y	0.0	0.1	2.8	0.9	0.0
65y+	0.0	0.0	0.1	0.0	0.0

Table A4.4 Others contact matrix. Daily number contacts by age group at other locations.

	0-4y	5-17y	18-49y	50-64y	65y+
0-4y	0.7	0.7	1.8	0.6	0.3
5-17y	0.2	2.6	2.1	0.4	0.2
18-49y	0.1	0.7	3.3	0.6	0.2
50-64y	0.1	0.3	2.2	1.1	0.4
65y+	0.0	0.2	1.3	0.8	0.6

Estimation of age-stratified proportion of population at high-risk for COVID-10 complications

We estimate age-specific proportions of the population at high risk of complications from COVID-19 based on data for Austin, TX and Round-Rock, TX from the CDC's 500 cities project (Figure A2) [18]. We assume that high risk conditions for COVID-19 are the same as those specified for influenza by the CDC [14]. The CDC's 500 cities project provides city-specific estimates of prevalence for several of these conditions among adults [19]. The estimates were obtained from the 2015-2016 Behavioral Risk Factor Surveillance System (BRFSS) data using a small-area estimation methodology called multi-level regression and poststratification [15,16]. It links geocoded health surveys to high spatial resolution population demographic and socioeconomic data [16].

Estimating high-risk proportions for adults. To estimate the proportion of adults at high risk for complications, we use the CDC's 500 cities data, as well as data on the prevalence of HIV/AIDS, obesity and pregnancy among adults (Table A6).

The CDC 500 cities dataset includes the prevalence of each condition on its own, rather than the prevalence of multiple conditions (e.g., dyads or triads). Thus, we use separate co-morbidity estimates to determine overlap. Reference about chronic conditions [20] gives US estimates for the proportion of the adult population with 0, 1 or 2+ chronic conditions, per age group. Using this and the 500 cities data we can estimate the proportion of the population p_{HR} in each age group in each city with at least one chronic condition listed in the CDC 500 cities data (Table A6) putting them at high-risk for flu complications.

HIV: We use the data from table 20a in CDC HIV surveillance report [21] to estimate the population in each risk group living with HIV in the US (last column, 2015 data). Assuming independence between HIV and other chronic conditions, we increase the proportion of the population at high-risk for influenza to account for individuals with HIV but no other underlying conditions.

Morbid obesity: A BMI over 40kg/m^2 indicates morbid obesity, and is considered high risk for influenza. The 500 Cities Project reports the prevalence of obese people in each city with BMI over 30kg/m^2 (not necessarily morbid obesity). We use the data from table 1 in Sturm and Hattori [22] to estimate the proportion of people with BMI>30 that actually have BMI>40 (across the US); we then apply this to the 500 Cities obesity data to estimate the proportion of people who are morbidly obese in each city. Table 1 of Morgan et al. [23] suggests that 51.2% of morbidly obese adults have at least one other high risk chronic condition, and update our high-risk population estimates accordingly to account for overlap.

Pregnancy: We separately estimate the number of pregnant women in each age group and each city, following the methodology in CDC reproductive health report [24]. We assume independence between any of the high-risk factors and pregnancy, and further assume that half the population are women.

Estimating high-risk proportions for children. Since the 500 Cities Project only reports data for adults 18 years and older, we take a different approach to estimating the proportion of children at high risk for severe influenza. The two most prevalent risk factors for children are asthma and obesity; we also account for childhood diabetes, HIV and cancer.
From Miller et al. [25], we obtain national estimates of chronic conditions in children. For asthma, we assume that variation among cities will be similar for children and adults. Thus, we use the relative prevalences of asthma in adults to scale our estimates for children in each city. The prevalence of HIV and cancer in children are taken from CDC HIV surveillance report [21] and cancer research report [26], respectively.

We first estimate the proportion of children having either asthma, diabetes, cancer or HIV (assuming no overlap in these conditions). We estimate city-level morbid obesity in children using the estimated morbid obesity in adults multiplied by a national constant ratio for each age group estimated from Hales et al. [27], this ratio represents the prevalence in morbid obesity in children given the one observed in adults. From Morgan et al. [23], we estimate that 25% of morbidly obese children have another high-risk condition and adjust our final estimates accordingly.

Resulting estimates. We compare our estimates for the Austin-Round Rock Metropolitan Area to published national-level estimates [28] of the proportion of each age group with underlying high risk conditions (Table A6). The biggest difference is observed in older adults, with Austin having a lower proportion at risk for complications for COVID-19 than the national average; for 25-39 year olds the high risk proportion is slightly higher than the national average.

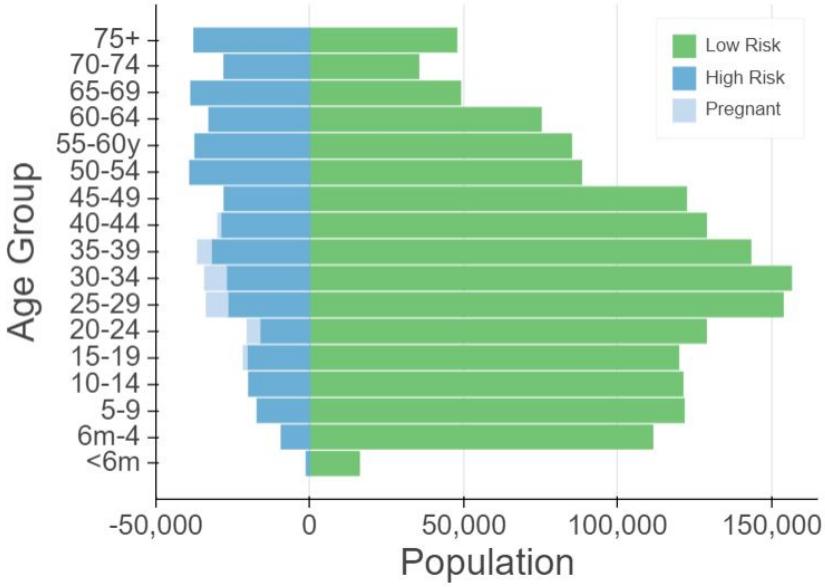

Figure A2. Demographic and risk composition of the Austin-Round Rock MSA. Bars indicate age-specific population sizes, separated by low risk, high risk, and pregnant. High risk is defined as individuals with cancer, chronic kidney disease, COPD, heart disease, stroke, asthma, diabetes, HIV/AIDS, and morbid obesity, as estimated from the CDC 500 Cities Project [18] reported HIV prevalence [21] and reported morbid obesity prevalence [22,23] corrected for multiple conditions. The population of pregnant women is derived using the CDC's method combining fertility, abortion and fetal loss rates [29–31].

Table A6. High-risk conditions for influenza and data sources for prevalence estimation

Condition	Data source
Cancer (except skin), chronic kidney disease, COPD, coronary heart disease, stroke, asthma, diabetes	CDC 500 cities [18]
HIV/AIDS	CDC HIV Surveillance report [21]
Obesity	CDC 500 cities [18], Sturm and Hattori [22], Morgan et al.[23]
Pregnancy	National Vital Statistics Reports [29] and abortion data [30]

Table A7: Comparison between published national estimates and Austin-Round Rock MSA estimates of the percent of the population at high-risk of influenza/COVID-19 complications.

Age Group	National estimates [27]	Austin (excluding pregnancy)	Pregnant women (proportion of age group)
0 to 6 months	NA	6.8	-
6 months to 4 years	6.8	7.4	-
5 to 9 years	11.7	11.6	-
10 to 14 years	11.7	13.0	-
15 to 19 years	11.8	13.3	1.7
20 to 24 years	12.4	10.3	5.1
25 to 34 years	15.7	13.5	7.8
35 to 39 years	15.7	17.0	5.1
40 to 44 years	15.7	17.4	1.2
45 to 49 years	15.7	17.7	-
50 to 54 years	30.6	29.6	-
55 to 60 years	30.6	29.5	-
60 to 64 years	30.6	29.3	-
65 to 69 years	47.0	42.2	-
70 to 74 years	47.0	42.2	-
75 years and older	47.0	42.2	-

References

1. COVID-19 Risk-Based Guidelines | AustinTexas.gov. [cited 18 May 2020]. Available: http://www.austintexas.gov/page/covid-19-risk-based-guidelines

2. Keeling MJ, Rohani P. Modeling Infectious Diseases in Humans and Animals. Princeton University Press; 2011.

3. Gillespie DT. Approximate accelerated stochastic simulation of chemically reacting systems. J Chem Phys. 2001;115: 1716–1733.

4. Ionides EL, Nguyen D, Atchadé Y, Stoev S, King AA. Inference for dynamic and

latent variable models via iterated, perturbed Bayes maps. Proc Natl Acad Sci U S A. 2015;112: 719–724.

5. King AA, Nguyen D, Ionides EL. Statistical Inference for Partially Observed Markov Processes via the R Package pomp. arXiv [stat.ME]. 2015. Available: http://arxiv.org/abs/1509.00503

6. Halfin S, Whitt W. Heavy-Traffic Limits for Queues with Many Exponential Servers. Oper Res. 1981;29: 567–588.

7. Duque D, Morton DP, Singh B, Du Z, Pasco R, Meyers LA. COVID-19: How to Relax Social Distancing If You Must. medRxiv. 2020. Available: https://www.medrxiv.org/content/10.1101/2020.04.29.20085134v1.abstract

8. minimize(method='trust-constr') — SciPy v1.4.1 Reference Guide. [cited 19 Apr 2020]. Available: https://docs.scipy.org/doc/scipy/reference/optimize.minimize-trustconstr.html

9. He X, Lau EHY, Wu P, Deng X, Wang J, Hao X, et al. Temporal dynamics in viral shedding and transmissibility of COVID-19. Nat Med. 2020. doi:10.1038/s41591-020-0869-5

10. Gudbjartsson DF, Helgason A, Jonsson H, Magnusson OT, Melsted P, Norddahl GL, et al. Spread of SARS-CoV-2 in the Icelandic Population. N Engl J Med. 2020. doi:10.1056/NEJMoa2006100

11. Zhang J, Litvinova M, Wang W, Wang Y, Deng X, Chen X, et al. Evolving epidemiology and transmission dynamics of coronavirus disease 2019 outside Hubei province, China: a descriptive and modelling study. Lancet Infect Dis. 2020. doi:10.1016/S1473-3099(20)30230-9

12. He D, Zhao S, Lin Q, Zhuang Z, Cao P, Wang MH, et al. The relative transmissibility of asymptomatic COVID-19 infections among close contacts. Int J Infect Dis. 2020;94: 145–147.

13. Verity R, Okell LC, Dorigatti I, Winskill P, Whittaker C, Imai N, et al. Estimates of the severity of COVID-19 disease. Epidemiology. medRxiv; 2020. doi:10.1101/2020.03.09.20033357

14. CDC. People at High Risk of Flu. In: Centers for Disease Control and Prevention [Internet]. 1 Nov 2019 [cited 26 Mar 2020]. Available: https://www.cdc.gov/flu/highrisk/index.htm

15. CDC - BRFSS. 5 Nov 2019 [cited 26 Mar 2020]. Available: https://www.cdc.gov/brfss/index.html

16. Zhang X, Holt JB, Lu H, Wheaton AG, Ford ES, Greenlund KJ, et al. Multilevel

regression and poststratification for small-area estimation of population health outcomes: a case study of chronic obstructive pulmonary disease prevalence using the behavioral risk factor surveillance system. Am J Epidemiol. 2014;179: 1025–1033.

17. Tindale L, Coombe M, Stockdale JE, Garlock E, Lau WYV, Saraswat M, et al. Transmission interval estimates suggest pre-symptomatic spread of COVID-19. Epidemiology. medRxiv; 2020. doi:10.1101/2020.03.03.20029983

18. 500 Cities Project: Local data for better health | Home page | CDC. 5 Dec 2019 [cited 19 Mar 2020]. Available: https://www.cdc.gov/500cities/index.htm

19. Health Outcomes | 500 Cities. 25 Apr 2019 [cited 28 Mar 2020]. Available: https://www.cdc.gov/500cities/definitions/health-outcomes.htm

20. Part One: Who Lives with Chronic Conditions. In: Pew Research Center: Internet, Science & Tech [Internet]. 26 Nov 2013 [cited 23 Nov 2019]. Available: https://www.pewresearch.org/internet/2013/11/26/part-one-who-lives-with-chronic-conditions/

21. for Disease Control C, Prevention, Others. HIV surveillance report. 2016; 28. URL: http://www cdc gov/hiv/library/reports/hiv-surveil-lance html Published November. 2017.

22. Sturm R, Hattori A. Morbid obesity rates continue to rise rapidly in the United States. Int J Obes . 2013;37: 889–891.

23. Morgan OW, Bramley A, Fowlkes A, Freedman DS, Taylor TH, Gargiullo P, et al. Morbid obesity as a risk factor for hospitalization and death due to 2009 pandemic influenza A(H1N1) disease. PLoS One. 2010;5: e9694.

24. Estimating the Number of Pregnant Women in a Geographic Area from CDC Division of Reproductive Health. Available: https://www.cdc.gov/reproductivehealth/emergency/pdfs/PregnacyEstimatoBrochure508.pdf

25. Miller GF, Coffield E, Leroy Z, Wallin R. Prevalence and Costs of Five Chronic Conditions in Children. J Sch Nurs. 2016;32: 357–364.

26. Cancer Facts & Figures 2014. [cited 30 Mar 2020]. Available: https://www.cancer.org/research/cancer-facts-statistics/all-cancer-facts-figures/cancer-facts-figures-2014.html

27. Hales CM, Fryar CD, Carroll MD, Freedman DS, Ogden CL. Trends in Obesity and Severe Obesity Prevalence in US Youth and Adults by Sex and Age, 2007-2008 to 2015-2016. JAMA. 2018;319: 1723–1725.

28. Zimmerman RK, Lauderdale DS, Tan SM, Wagener DK. Prevalence of high-risk indications for influenza vaccine varies by age, race, and income. Vaccine. 2010;28: 6470–6477.

29. Martin JA, Hamilton BE, Osterman MJK, Driscoll AK, Drake P. Births: Final Data for 2017. Natl Vital Stat Rep. 2018;67: 1–50.

30. Jatlaoui TC, Boutot ME, Mandel MG, Whiteman MK, Ti A, Petersen E, et al. Abortion Surveillance - United States, 2015. MMWR Surveill Summ. 2018;67: 1–45.

31. Ventura SJ, Curtin SC, Abma JC, Henshaw SK. Estimated pregnancy rates and rates of pregnancy outcomes for the United States, 1990-2008. Natl Vital Stat Rep. 2012;60: 1–21.